Anatomic Changes in Schlemm's Canal and Collector Channels in Normal and Primary Open-Angle Glaucoma Eyes Using Low and High Perfusion Pressures

Cheryl R. Hann,[1] Andrew J. Vercnocke,[2] Michael D. Bentley,[3] Steven M. Jorgensen,[2] and Michael P. Fautsch[1]

[1]Department of Ophthalmology, Mayo Clinic, Rochester, Minnesota, United States
[2]Department of Physiology and Biomedical Engineering, Mayo Clinic, Rochester, Minnesota, United States
[3]Department of Biological Sciences, Minnesota State University, Mankato, Minnesota, United States

Correspondence: Michael P. Fautsch, Department of Ophthalmology, Mayo Clinic, 200 First Street SW, Rochester, MN 55905, USA; fautsch@mayo.edu.

Submitted: February 10, 2014
Accepted: August 5, 2014

Citation: Hann CR, Vercnocke AJ, Bentley MD, Jorgensen SM, Fautsch MP. Anatomic changes in Schlemm's canal and collector channels in normal and primary open-angle glaucoma eyes using low and high perfusion pressures. *Invest Ophthalmol Vis Sci*. 2014;55:5834–5841. DOI:10.1167/iovs.14-14128

Purpose. To examine the anatomy of Schlemm's canal (SC) and collector channels (CCs) in normal human and primary open-angle glaucoma (POAG) eyes under low and high perfusion pressure.

Methods. In normal ($n = 3$) and POAG ($n = 3$) eye pairs, one eye was perfused at 10 mm Hg while the fellow eye was perfused at 20 mm Hg for 2 hours. Eyes were perfusion fixed at like pressures, dissected into quadrants, embedded in Epon Araldite, and scanned by three-dimensional micro-computed tomography (3D micro-CT). Schlemm's canal volume, CC orifice area, diameter, and number were measured using ANALYZE software.

Results. Normal eyes showed a larger SC volume (3.3-fold) and CC orifice area (9962.8 vs. 8825.2 μm^2) and a similar CC diameter (34.3 $\pm$ 17.8 vs. 32.7 $\pm$ 13.0 μm) at 10 mm Hg compared to 20 mm Hg. In POAG eyes, SC volume (2.0-fold), CC orifice area (8049.2μm^2–6468.4 μm^2), and CC diameter (36.2 $\pm$ 19.1 vs. 29.0 $\pm$ 13.8 μm) were increased in 10 mm Hg compared to 20 mm Hg perfusion pressures. Partial and total CC occlusions were present in normal and POAG eyes, with a 3.7-fold increase in total occlusions in POAG eyes compared to normal eyes at 20 mm Hg. Visualization of CCs increased by 24% in normal and by 21% in POAG eyes at 20 mm Hg compared to 10 mm Hg. Schlemm's canal volume, CC area, and CC diameter were decreased in POAG eyes compared to normal eyes at like pressures.

Conclusions. Compensatory mechanisms for transient and short periods of increased pressure appear to be diminished in POAG eyes. Variable response to pressure change in SC and CCs may be a contributing factor to outflow facility change in POAG eyes.

Keywords: Schlemm's canal, collector channel, POAG, glaucoma, anterior segment

In glaucoma, chronic elevation of pressure in the anterior segment of the eye causes irreversible damage to the optic nerve head resulting in blindness. While a reduced rate of aqueous humor removal from the anterior chamber is responsible for pressure elevation, the specific cause of this impediment remains elusive despite rigorous investigation.[1] In the conventional outflow pathway, resistance to outflow is thought to be located in the region of Schlemm's canal (SC) endothelium, its basement membrane, and the juxtacanalicular tissue (JCT) of the trabecular meshwork.[2–4] Under elevated pressure, multiple changes occur within this region in normal human eyes. These include an increase in giant vacuole size and numbers,[5–8] an increase in JCT empty space due to ciliary muscle contraction, and a luminal decrease of SC.[9–11] With continued pressure elevation, focal regions of collapse within SC have been observed.[5,9] Up to 50% of outflow resistance has been attributed to SC, collector channels (CCs), and the episcleral venous system at low perfusion pressures, and lesser but significant outflow resistance effects due to these components at higher perfusion pressures.[12]

Early investigations and more recent optical coherence tomography studies analyzing primary open-angle glaucoma (POAG) eyes found decreased SC cross-sectional area, perimeter, and length.[13–16] Histopathologic changes to the outer wall in POAG include increased collapse and narrowing of CCs and intrascleral veins along with adhesion of SC endothelium to CC orifice walls and herniation of JCT with blockage of CC orifices (Gong H, et al. *IOVS* 2007;48:ARVO E-Abstract 2079).[17–19] These changes in POAG eyes identify SC and CCs as important anatomic structures for the study of resistance mechanisms to aqueous outflow.

Our laboratory and others have demonstrated the existence of preferential flow pathways adjacent to CCs.[20–24] This work has given impetus to the investigation of inner wall and outer wall regions immediately adjacent to and surrounding these areas. The inner wall of SC is linked to the outer wall of SC through septal bridges that are often present adjacent to CC orifices.[25] Additionally, the outer wall endothelium, CC orifices, and CC walls all are buttressed at the base of their endothelial cells with an elastic-like sheath and tendon network similar to the one adjacent to the inner wall, which supports and allows for distensibility of the inner wall endothelium.[26–28] These observations suggest that the inner wall and outer wall may respond in a similar manner to maintain homeostatic fluid flow through this region. However, studies investigating the response of the

Table. Clinical Characteristics of Normal and Glaucoma Tissue

Specimens	Age/Sex	Eye History
Normal 1	63/M	None available
Normal 2	61/F	None available
Normal 3	63/F	Cataracts bilateral; diabetes
POAG 1	88/F	Glaucoma, 8 y; diabetes; bilateral IOLs; Xalatan, Timoptic. Pressures at diagnosis, R 18: L 18. Last recorded IOPs, R 15: L 15. Cup/disc ratio, R 0.8/L 0.4.
POAG 2	61/M	Glaucoma, 2 y; Alphagan, Xalatan. Pressures at diagnosis, R 14: L 16. Last recorded IOPs, R 12: L 13. Cup/disc ratio, R 0.09/L 0.95.
POAG 3	84/M	Glaucoma, 3 y; diabetes; bilateral IOLs; Xalatan; diabetic retinopathy, bilateral. Pressures at diagnosis, R 14: L 14. Last recorded IOPs, R 12: L 10. Cup/disc ratio, R 0.7/L 0.75.

conventional outflow pathway with reference to changes in the outer wall and distal outflow system in normal and POAG eyes under low and high pressure have not been performed.

Study of the SC as a functional entity with its associated CCs under changing pressure has not been feasible due to technical challenges of viewing these structures in three dimensions. Our laboratory has established three-dimensional micro-computed tomography (3D micro-CT) as a viable method to study the outflow pathway as a complete anatomic unit.[27] Three-dimensional micro-CT enables 3D reconstruction of SC and CCs to view them in the context of the entire aqueous outflow pathway, enabling reconstruction and examination under varying pressures. Images obtained by 3D micro-CT show strong similarity to description of CC locations in previous reports following laborious serial sectioning and reconstruction of the distal outflow pathway.[18] The purpose of this study was to determine and compare the anatomic changes occurring to SC and CCs in normal and POAG eyes under low and high perfusion pressure.

Methods

Perfusion Studies

Three pairs of normal human eyes (ages 61, 63, 68) and three pairs of POAG eyes (ages 61, 84, 88) were obtained from the Minnesota Lions Eye Bank (Minneapolis, MN, USA) (Table). For 2 hours, one eye of each pair was perfused at 10 mm Hg (low pressure) and the fellow eye was perfused at 20 mm Hg (high pressure) with phosphate-buffered saline containing 5.5 mM glucose.[29] Each eye was fixed at the assigned initial perfusion pressure with 4% paraformaldehyde/2% glutaraldehyde in 0.1 M phosphate buffer for 8 to 12 hours. The anterior segment was removed and divided into quadrants. All quadrants were rinsed in 0.1 M phosphate buffer, fixed in 2% osmium tetroxide, dehydrated in an ascending series of ethanol, and embedded in Epon Araldite (Electron Microscopy Sciences, Hatfield, PA, USA). All quadrants of normal eyes (12 low pressure; 12 high pressure) and all quadrants of POAG eyes (12 low pressure; 12 high pressure) were analyzed in their entirety for this study.

3D Micro-CT Analysis

Each quadrant was mounted on a 360° rotating stage and scanned at 6-μm voxel resolution using a molybdenum X-ray source as previously described.[27] Five subregion blocks from selected quadrants with elevated CC numbers observed at 6 μm were scanned for CC confirmation at higher resolution (2 μm) using the synchrotron x-ray at the National Synchrotron Light Source in Brookhaven, New York.

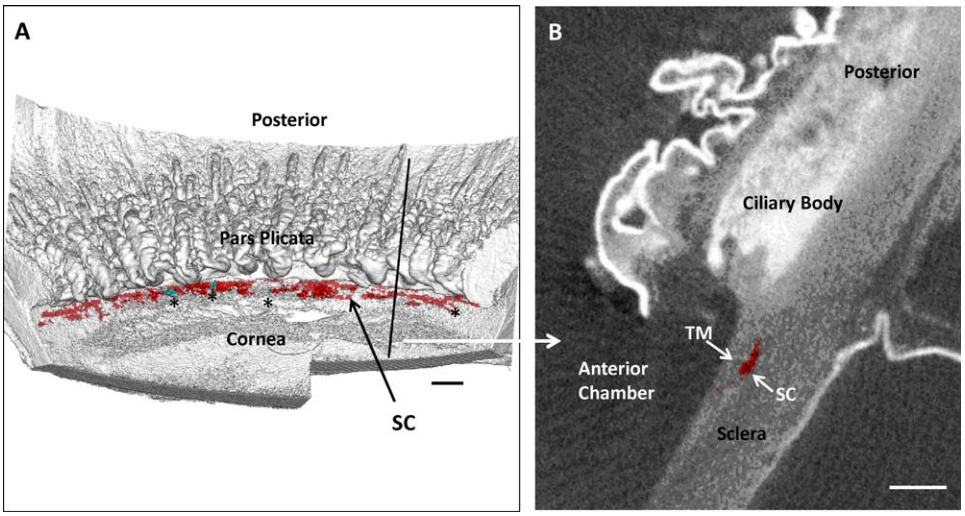

Figure 1. Analysis of Schlemm's canal (SC) and collector channels (CCs) within the distal outflow pathway. (**A**) Three-dimensional micro-CT reconstruction of a nasal quadrant from one of the primary open-angle glaucoma (POAG) eyes in the study. The quadrant reconstruction is oriented with the corneal endothelial surface up. Ciliary body processes of the pars plicata are visible posterior to Schlemm's canal (SC), which is shown in *red*. Collector channel orifices are shown in *bright aqua* and are indicated with *black asterisks*. A *vertical black line* indicates where a radial section was removed from the volume for (**B**). *Scale bar*: 500 μm. (**B**) A 6-μm radial section from 3D micro-CT volume shown in (**A**) at *black vertical line*. Schlemm's canal lumen is shown in *red. Scale bar*: 500 μm. TM, trabecular meshwork.

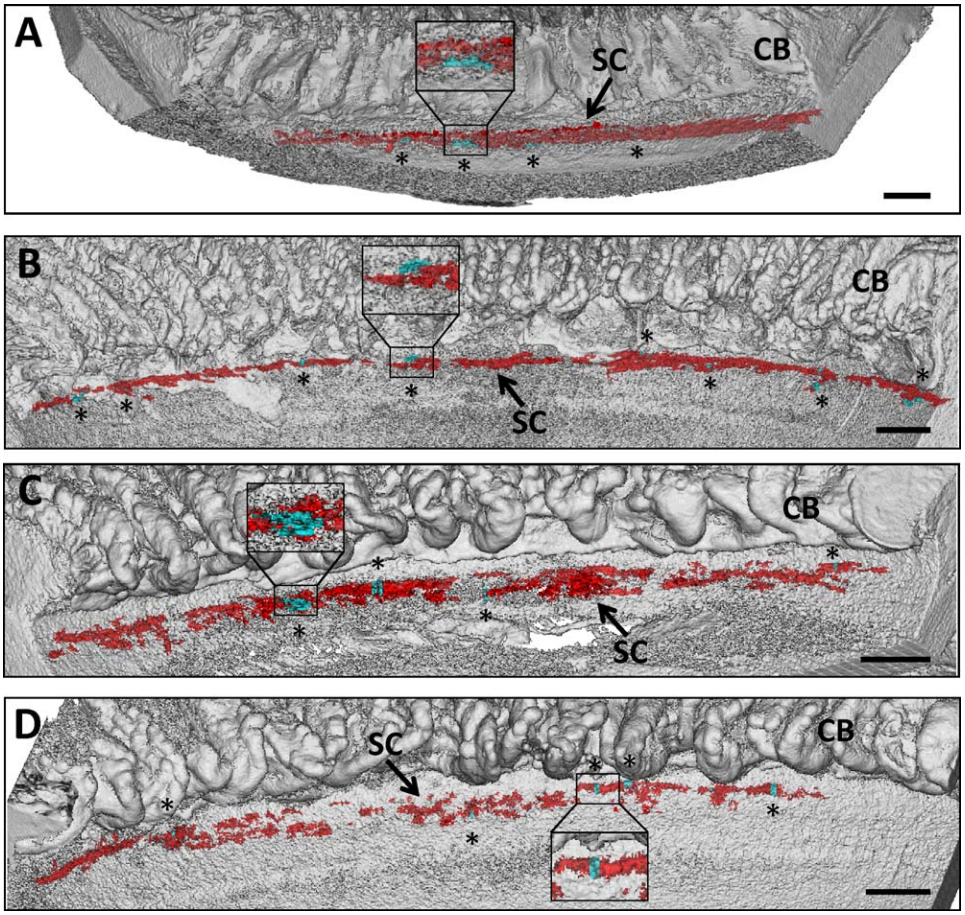

FIGURE 2. Three-dimensional micro-CT reconstruction of SC and CCs. (**A**) Three-dimensional reconstruction of 6-μm 3D micro-CT images of a nasal quadrant wedge isolated from a normal eye perfused at 10 mm Hg. Four CCs (*aqua* and *asterisks*) were identified in the serpentine-appearing SC (*red*) anterior to ciliary body (CB). *Inset* shows CC orifice opening in SC. (**B**) Three-dimensional reconstruction of 6-μm 3D micro-CT images of a nasal quadrant wedge from the fellow eye in (**A**) perfused at 20 mm Hg. Schlemm's canal (*red*) becomes more discontinuous and displays less anastomotic areas at elevated pressure. Eight CCs (*aqua* and *asterisks*) are identified in this wedge. (**C**) Three-dimensional reconstruction of 6-μm 3D micro-CT images of a superior quadrant wedge isolated from a POAG eye perfused at 10 mm Hg. Schlemm's canal appears more discontinuous than in normal eyes perfused at 10 mm Hg, and anastomosing channels are less frequent. Four CC orifices (*aqua* and *asterisks*) were identified anterior to ciliary body (CB). (**D**) Three-dimensional reconstruction of 6-μm 3D micro-CT images of a superior quadrant wedge from the fellow eye in (**C**) perfused at 20 mm Hg. Schlemm's canal (*red*) becomes more discontinuous, and adherent areas between inner and outer wall are more prevalent. Five CCs (*aqua* and *asterisks*) are identified in this wedge. (**A–D**) *Inset* shows magnified representative CC. *Scale bars*: 1000 μm.

Quantitative Assessment of 3D Micro-CT Volumes

Each quadrant volume (Fig. 1A) was viewed using the multiplanar section module within ANALYZE (Biomedical Imaging Resource; Mayo Clinic, Rochester, MN, USA), a software package developed for the analysis and 3D reconstruction of medical imaging modalities[30] to locate SC and CCs. This allowed the quadrant volume data to be viewed in 6-μm sections (Fig. 1B). Schlemm's canal was identified from abrupt grayscale differences, with fluid-containing areas represented by black regions and the surrounding tissue appearing as light gray. Collector channels were identified as openings that extended from the outer wall of SC into the sclera using parameters established from several labs, including ours, where we confirmed CCs by 3D micro-CT and validated their presence by correlative serial sections stained with toluidine blue.[18,27,31] Briefly, CCs were identified as openings in the outer wall of SC with orifices having a funnel or tubular shape with varying sizes between 10 and 100 μm. Collector channel orifices had to have an observable connection with vessels adjacent to SC before they were counted as a CC. In the multiplanar mode of ANALYZE, CCs were identified, traced, and segmented from the quadrant volume (Fig. 1B). Orifice diameters were measured at the midpoint of the CC volume. The CC orifice areas were analyzed by triangulating on the center orifice slice and the slice adjacent to it, creating an oblique section at the orifice and measuring the area in the region of interest module using ANALYZE.

The 3D volume images of SC and CCs were created as separate object maps from the quadrant volumes using ANALYZE. The volume of SC was measured using the stereology module in ANALYZE.[32] The 3D volume images of SC and CCs were viewed in quadrant or complete anterior segment renderings.

Correlative Studies by Light Microscopy

Correlative studies were done using light microscopy to address boundaries of 3D micro-CT to effectively evaluate CC number and size. Five subregions obtained from two normal eyes perfused at 20 mm Hg were scanned at 6 and 2 μm by 3D micro-CT. One thousand 1-μm serial radial sections were cut from each selected subregion ($n = 5$), and all 5000 sections were stained with toluidine blue and examined by light

microscopy. A total of 34 CCs were identified and evaluated in normal eyes (24 open CCs, 9 CCs with partial occlusion, and 1 CC with total occlusion). Correlative sections and previous reports confirmed CC orifice size range from 10 to 100 μm and volumes from 10 to 70 μm^3.[18,21,25,27] Collector channels identified by 3D micro-CT with diameters between 10 and 100 μm and with volumes between 10 and 70 μm^3 were included in this analysis. Total CC numbers used for diameter and area calculations were as follows: normal 10 mm Hg, 77; normal 20 mm Hg, 105; POAG 10 mm Hg, 79; and POAG 20 mm Hg, 79.

Occlusions in CCs were identified as either open (open or partially occluded) or totally occluded. Partially occluded CCs displayed the presence of SC inner wall distension and adhesion into the orifice, and/or the presence of some occlusive material within the CC orifice. Total occlusion consisted of complete blockage of the lumen and the CC orifice by SC inner wall and/or occlusive material.

Statistics

Values are expressed as mean ± standard deviation. Differences in CC numbers between low and high perfusion pressure eyes were compared using paired *t*-test. Results were considered significant when $P \leq 0.05$.

Results

Normal eyes perfused at 10 mm Hg showed a continuous serpentine SC with anastomosing channels (Fig. 2A) similar to those previously reported.[31,33,34] This pattern was maintained at 20 mm Hg, but SC appeared more often as a single channel with less continuity (Fig. 2B). The anatomic change in SC was reflected in volume; 20 mm Hg perfused eyes (6.7 μm^3) had a 3.3-fold decrease in SC volume when compared to 10 mm Hg perfused eyes (22.0 μm^3). In contrast, POAG eyes at 10 mm Hg showed short lengths of SC with variable anastomotic-like regions (Fig. 2C). This pattern was also seen at 20 mm Hg, with more pronounced SC discontinuity and a reduction in anastomotic-like regions (Fig. 2D). Areas with inner and outer walls in close apposition were observed more frequently at 20 mm Hg, indicating areas of canal narrowing, collapse, adhesion, or occlusion. In POAG eyes, the average area at 10 mm Hg was 7.0 μm^3, decreasing to 3.0 μm^3 at 20 mm Hg. In POAG eyes, areas with larger SC volume tended to contain open CCs compared to the narrower SC regions that were found between CC orifices.

Collector channels in normal and POAG eyes were located throughout the quadrants with no discernible pattern (Figs. 2A–D). The majority of CCs had funnel-like and tubular-shaped orifices, with diameters between 20 and 40 μm most commonly observed (Fig. 3). Some CCs joined intrascleral vessels that paralleled SC. Other CCs had small orifice diameters (10–20 μm) that extended short distances into paralleling vessels (Figs. 3C, 3D). Portions of the plexus adjacent to the outer wall of SC were infrequently observed.

Total CC numbers were compared in normal and POAG eyes. In normal eyes, 28.3 ± 18.3 CCs were identified in 10 mm Hg perfused eyes (Fig. 4). The number of CCs in each paired normal eye perfused at 20 mm Hg increased 24.2% to an average of 37.3 ± 13.1 CCs/eye ($P = 0.13$). In POAG eyes, a similar trend occurred; 27.7 ± 10.7 CCs/eye were identified in 10 mm Hg perfused eyes, and the number of visualized CCs increased in 20 mm Hg perfused eyes by 20.9% to 35.0 ± 8.2 CCs/eye ($P = 0.07$). Total occluded CCs were observed and confirmed in both normal and POAG eyes (Fig. 5). In normal eyes, 9.4% of CCs (8 of 85 CCs) were totally occluded at 10 mm Hg while 6.3% of CCs (7 of 112 CCs) were totally occluded at 20 mm Hg. Similar results were seen in POAG eyes perfused at 10 mm Hg, with 7.2% of CCs (6 of 83 CCs) totally occluded. In contrast, 24.8% of CCs (26 of 105) in POAG eyes perfused at 20 mm Hg were totally occluded. Considering that totally occluded CCs will have at minimum reduced ability to move fluid, comparison of open CCs (excluding total occlusions) in normal eyes showed CC numbers increased by 26.6% from 10 mm Hg (25.7 ± 14.8 CCs/eye) to 20 mm Hg (35.0 ± 13.1, $P = 0.02$) while POAG eyes showed negligible change in CC numbers (2.3%) from 10 mm Hg (25.7 ± 10.7) to 20 mm Hg (26.3 ± 8.5, $P = 0.85$).

While CC numbers increased in normal eyes with increasing perfusion pressure, average orifice diameter remained unchanged but CC orifice area decreased. In normal eyes, CC orifice diameter was 34.3 ± 17.8 μm at 10 mm Hg but slightly decreased to 32.7 ± 13.0 μm at 20 mm Hg. Collector channel orifice area decreased by 11.4% from 9962.8 μm^2 in 10 mm Hg

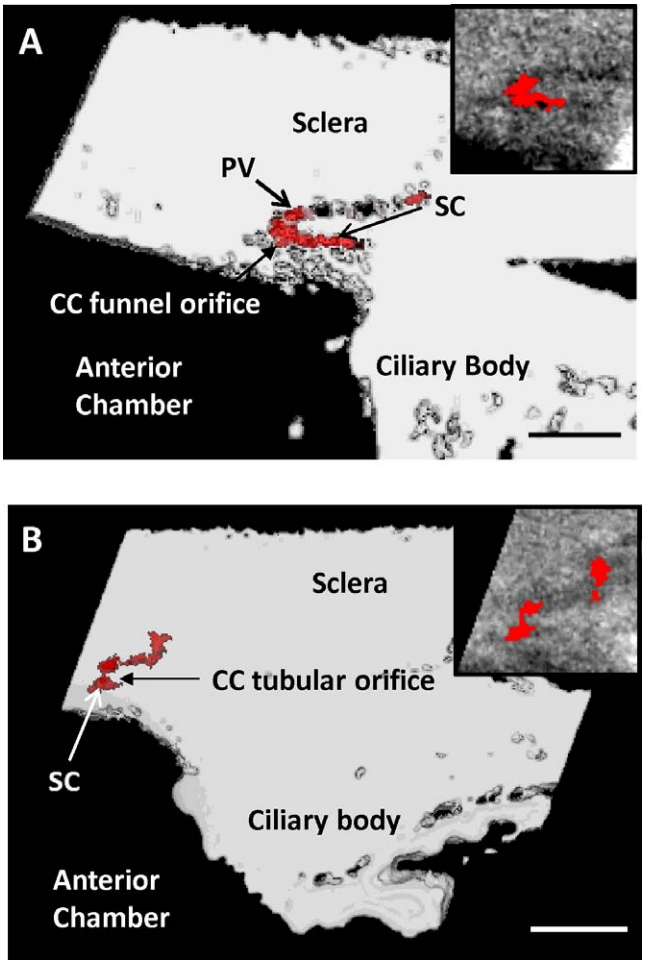

Figure 3. Types of CC orifices. (**A**) Three-dimensional micro-CT volume of SC with a funnel-shaped CC orifice that extends from middle of SC and travels posteriorly. A portion of the intrascleral parallel vessel (PV) leading away from the orifice is visible. This type of orifice was always observed to be wider initially, then becoming narrower as it extended away from SC. *Inset* contains a single radial section (6 μm) from the surface of the 3D volume. (**B**) Three-dimensional micro-CT volume of SC with a tubular-shaped CC orifice that extends a short distance and joins an intrascleral vessel traveling adjacent to SC. Collector channel orifices at SC and at connecting vessel are the same size. *Inset* contains a single radial 6-μm section from the surface of the volume showing the tubular orifice. *Scale bars*: 500 μm (**A**, **B**).

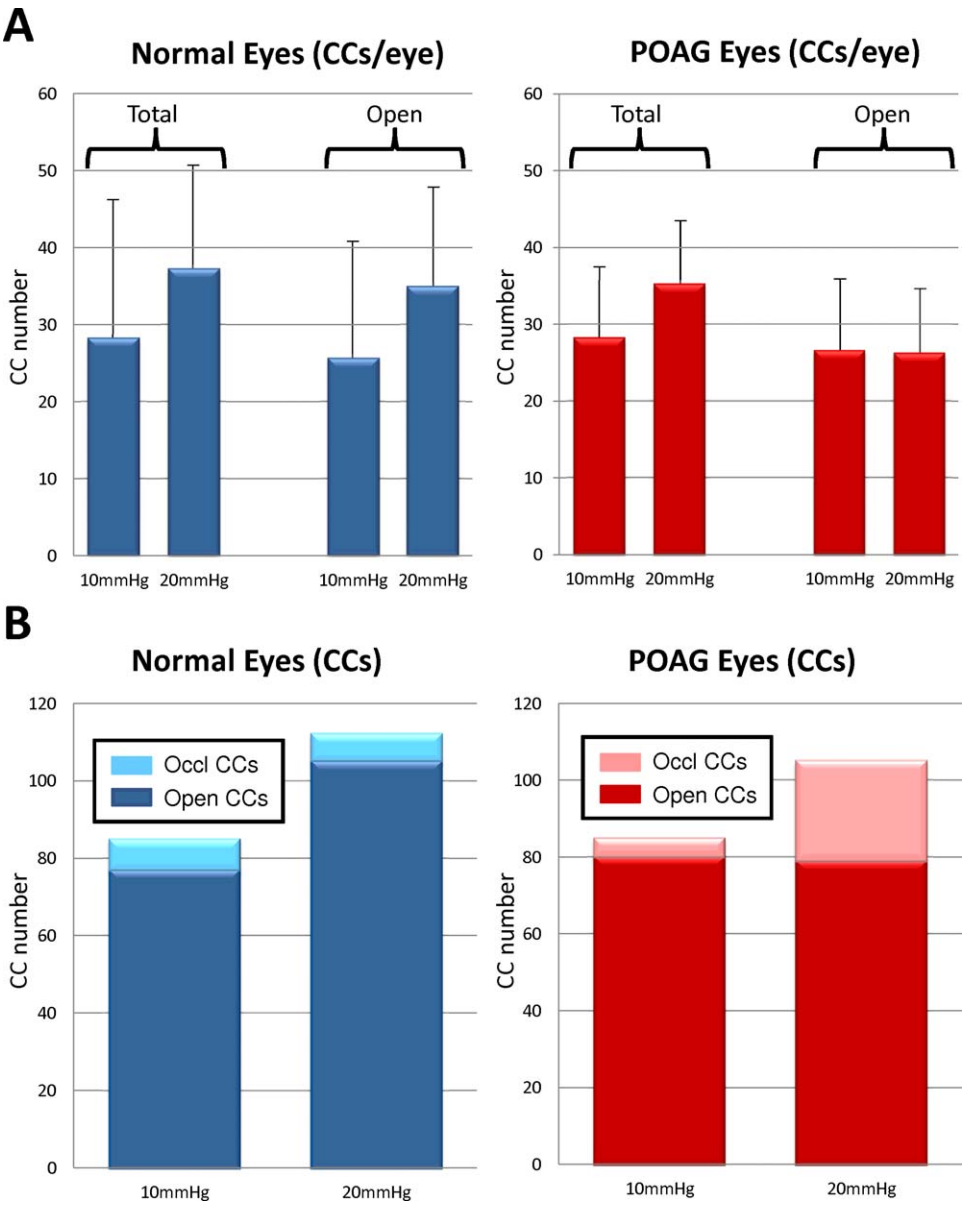

FIGURE 4. Collector channels in normal and POAG eyes. (**A**) Average number of CCs increases in normal ($n = 3$) and POAG ($n = 3$) eyes when pressure increases from 10 to 20 mm Hg. Number of open and partially open CCs increases in normal eyes from 10 to 20 mm Hg but does not change in POAG eyes. (**B**) Number of totally occluded CCs increases nearly 4-fold in POAG eyes at 20 mm Hg compared to normal eyes at 20 mm Hg.

normal eyes to 8825.2 μm^2 in 20 mm Hg normal eyes. In POAG eyes, CC orifice diameter decreased by 20% from 36.2 ± 19.1 um at 10 mm Hg to 29.0 ± 13.8 μm. A 19.7% decrease in CC orifice area was observed in POAG eyes (8049.2 μm^2 in 10 mm Hg eyes to 6468.4 μm^2 at 20 mm Hg).

DISCUSSION

The distal portion of the conventional outflow pathway is responsible for nearly 50% of outflow resistance in low-pressure perfused eyes. As perfusion pressure increases, the SC and CCs still contribute 30% of total outflow resistance through the conventional outflow pathway.[12] Even with the reported importance of the distal outflow pathway, no studies have compared the anatomic changes in SC and CCs at various pressures between normal and POAG eyes. This region has undergone minimal examination due to technical limitations in imaging the conventional outflow pathway as a whole. Using 3D micro-CT, we have compared the anatomic changes in SC and CCs in normal and POAG eyes using low (10 mm Hg) and high (20 mm Hg) perfusion pressures. In both normal and POAG eyes, SC and CCs were anatomically responsive to increases in perfusion pressure. In response to high pressure in normal eyes, SC volume and CC orifice area decreased while CC orifice diameter remained relatively constant. High pressure resulted in normal eyes having a 26.6% increase in observable open CCs. In POAG eyes, SC volume, CC diameter, and CC orifice area were decreased when pressure was elevated from 10 to 20 mm Hg. In contrast to findings in normal eyes, the number of open CCs in POAG eyes did not change between 10 and 20 mm Hg. Partial and total occlusions were present in normal eyes, but a greater number of total CC occlusions were observed in POAG eyes at high pressure.

Previous studies have reported 24 to 31 CCs in immersed eyes and 25 to 31 in low-pressure perfused specimens.[18,25] Our

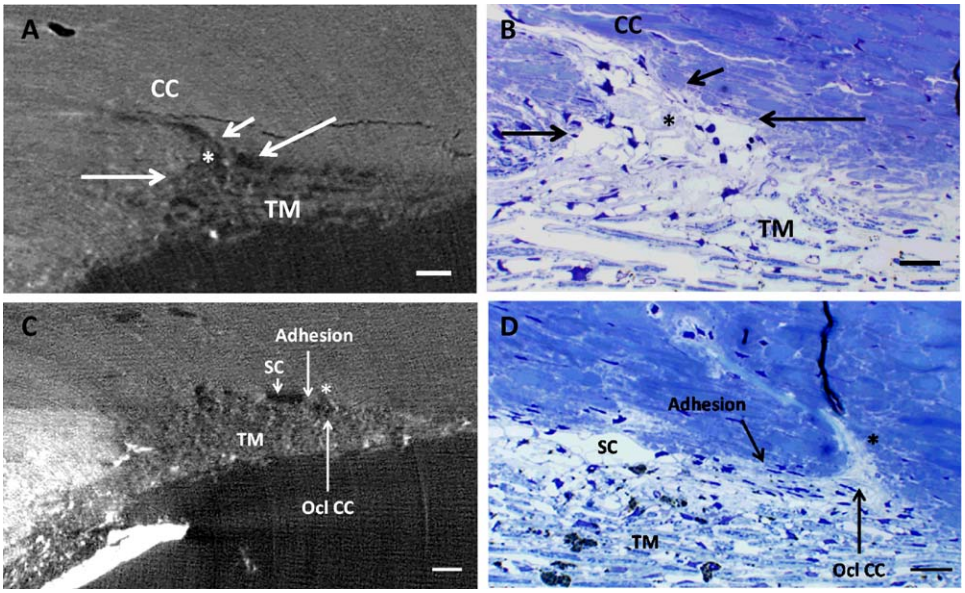

FIGURE 5. Juxtacanalicular expansion into CC orifice. (**A**) Three-dimensional micro-CT image (2 μm) showing JCT expansion (*asterisk*) into CC (imaged from eye perfused at 20 mm Hg). *Long arrows* indicate boundaries of CC orifice. Inner wall adhesion to outer wall of SC was observed in region just past the orifice (*short arrow*). (**B**). Correlative 1-μm plastic section of same region as in (**A**) with expanded JCT (*asterisk*), CC orifice (*long arrows*), and area of adhesion of JCT (*short arrow*) just past the orifice. Regions similar to this that were adherent in several sections but cleared were evaluated as open CCs. (**C**) Three-dimensional micro-CT images (2 μm) of an occluded CC (*asterisk*; imaged from eye perfused at 20 mm Hg), triangular in shape, and its orifice filled with *light gray* material. Area of adhesion can be seen posterior to occluded CC. (**D**) Correlative 1-μm toluidine blue–stained plastic section of (**C**) showing anterior CC (*asterisk*) filled with *light blue* occlusive material extending into the sclera. Area of adhesion can be seen posterior to the CC orifice. Ocl CC, occluded collector channel. *Scale bars*: 50 μm (**A**–**C**); 20 μm (**D**). TM, trabecular meshwork.

study found similar results in normal eyes perfused at 10 mm Hg with an average of 28.3 CCs per eye. The number of CCs increased to 37.3 in the contralateral eyes perfused at 20 mm Hg. While it is possible that distension of the tissue due to high pressure may have enlarged channels, making them easier to identify, we do not believe this was the case since CC orifice diameter at 20 mm Hg was nearly identical to that measured at 10 mm Hg.

While distension may have a small role in providing a means to image additional CCs at higher pressure, an alternative hypothesis is that some CCs at 10 mm Hg are inactive, obscured by flaps or outer wall undulations. As pressure increases (20 mm Hg), these flaps or outer wall undulations retract, opening up additional CCs, enabling increased fluid flow. Collector channels with lip-like and sieve-like structures at CC orifices have been reported.[31,35] An anatomic study done on CC orifice structure identified an additional type of complex orifice flap with fan-like structures that attached to both the inner wall and the outer wall (Bentley M, et al. *IOVS* 2012;53:ARVO E-Abstract 3234). This CC flap could be envisioned to move with the inner wall and outer wall, producing an open CC orifice under high pressure and, conversely, closing the CC orifice under low pressure. Change in outer wall undulations to a smooth profile at high pressure has also been reported.[36] Under this scenario, CCs may be part of a pressure-induced compensatory mechanism within the distal portion of the conventional outflow pathway. Although overall SC volume was reduced at high pressure, areas of open SC volume were generally associated with CCs. The reduced SC volume at high pressure is similar to observations in a study by Van Buskirk and Grant,[37] who found only a partial collapse of SC using perfusion at 20 mm Hg. This compensatory mechanism may serve to alleviate stress during acute rises in pressure but may become limited in chronic pressure elevation or increases in pressure past a certain threshold level. Experiments that can visualize CCs in real time are required to determine if some CCs are inactive due to flap closures but can respond to fluid flow under high pressure. Whether the change observed in CCs is a passive response to pressure or whether an active mechanosensitive response is required to activate the compensatory CCs will need to be determined.

Another observation from this study is that POAG eyes perfused at 10 mm Hg have SC dimensions similar to those of normal eyes perfused at 20 mm Hg. Normal eyes perfused at 20 mm Hg (6.7 μm^3) and POAG eyes perfused at 10 mm Hg (7.0 μm^3) had nearly identical SC volume and similar CC orifice area (8825.2 and 8049.2 μm^2). The percent of total occlusions was also similar between normal eyes perfused at 20 mm Hg (6.3%) and POAG eyes at 10 mm Hg (7.2%). This may indicate that occlusions observed in aging eyes are not reversible but are a permanent change. With aging, changes in the inner wall and outer wall during short bursts of high pressure, for example, during normal head movement and sneezing,[38] may occur with resistance due to apposition, fibrosis, and occlusion. The similarity of 10 mm Hg perfused pressure POAG eyes with high perfusion pressure normal eyes suggests that POAG eyes may have lost their ability to compensate for increased pressure through use of CCs from the reserve pool. Remodeling of the extracellular matrix in the inner and outer wall may reduce SC and CC elasticity, making this area less pliable and stiffer. Increased stiffness and extracellular matrix deposition have been reported in the trabecular meshwork in POAG eyes.[39,40] The loss of outer wall elasticity may explain the same number of nonoccluded CCs found in POAG eyes at 10 and 20 mm Hg, suggesting an inability of POAG eyes to compensate for pressure-induced changes. It is interesting to note that all three POAG patients were on various ocular hypotensive medications, yet none of the POAG eyes had SC and CC dimensions similar to those of normal eyes at low pressure.

Total occluded CCs were observed in normal and POAG eyes at both 10 and 20 mm Hg. While less than 10% of CCs had total occlusions in normal eyes at 10 and 20 mm Hg, total occlusions in POAG eyes were present in 24.8% of CCs at 20 mm Hg. The increased number of total occlusions in POAG eyes observed at higher perfusion pressures indicates that many of the CCs may be rendered partially or totally nonfunctional in POAG. Distension of the JCT into CC orifices has been observed under experimentally induced high pressure.[20,21] In normal eyes, distention of the inner wall may interfere only sporadically with CCs due to a large SC volume and reduced inner and outer wall juxtaposition. In POAG eyes, SC volume is reduced under high pressure, providing increased likelihood of apposition between inner and outer walls. This could lead to increase adhesion areas under elevated pressure, minimizing fluid flow and eventually resulting in totally occluded CCs. The occluding material may be a local production of extracellular material from aging SC endothelial cells, JCT cells, or CC endothelial cells. Characterization of the composition of the occlusive material may serve to identify its origin and provide an opportunity to interfere with its production and minimize its occlusive potential.

In summary, this study suggests that decreased outflow facility in POAG eyes may be due to a decrease in SC area and an increase in total occlusions resulting in a reduced number of open CCs available for fluid movement. Results also indicate a loss of adaptation in SC and CCs in POAG eyes to counteract an increase in pressure. While this study assessed nearly 200 CCs, it is limited due to the small number of individual eye pairs ($n =$ 3 normal and $n = 3$ POAG). Additionally, while all normal eyes were from individuals in their 60s, two pairs of the POAG eyes were from individuals in their 80s. This leaves open the possibility that some of the differences we observed were due to age-related changes. Future SC and CC three-dimensional studies in additional human eyes will help in further validating the anatomic changes in normal and POAG eyes under pressure, and to elucidate the function and contribution of the distal outflow pathway to outflow facility.

Acknowledgments

The authors thank Bob Highet of the Mayo Clinic Department of Engineering for expert technical assistance in the precise retrimming of tissue blocks in preparation for scanning at Brookhaven National Labs. Three-dimensional micro-CT imaging was performed at the National Synchrotron Light Source at Brookhaven National Laboratory in Upton, New York, United States.

Supported in part by National Institutes of Health Research Grants EY 07065 and EY 21727; Mayo Foundation, Rochester, Minnesota, United States; and Research to Prevent Blindness, New York, New York, United States. MPF is a recipient of a Lew R. Wasserman Merit Award, and the Department of Ophthalmology, Mayo Clinic, is the recipient of an unrestricted grant. The National Synchrotron Light Source is supported by the U.S. Department of Energy, Office of Science, Office of Basic Energy Sciences, under Contract No. DE-AC02-98CH10886.

Disclosure: **C.R. Hann**, None; **A.J. Vercnocke**, None; **M.D. Bentley**, None; **S.M. Jorgensen**, None; **M.P. Fautsch**, None

References

1. Chader GJ. Key needs and opportunities for treating glaucoma. *Invest Ophthalmol Vis Sci*. 2012;53:2456–2460.
2. Grant WM. Further studies on facility of flow through the trabecular meshwork. *AMA Arch Ophthalmol*. 1958;60:523–533.
3. Johnson M. What controls aqueous humor outflow? *Exp Eye Res*. 2006;82:545–557.
4. Overby DR, Stamer WD, Johnson M. The changing paradigm of outflow resistance generation: towards synergistic models of the JCT and inner wall endothelium. *Exp Eye Res*. 2009;88:656–670.
5. Grierson I, Lee WR. Changes in the monkey outflow apparatus at graded levels of intraocular pressure: a qualitative analysis by light microscopy and scanning electron microscopy. *Exp Eye Res*. 1974;19:21–33.
6. Grierson I, Lee WR. The fine structure of the trabecular meshwork at graded levels of intraocular pressure. (1) Pressure effects within the near-physiological range (8–30 mmHg). *Exp Eye Res*. 1975;20:505–521.
7. Grierson I, Lee WR. The fine structure of the trabecular meshwork at graded levels of intraocular pressure. (2) Pressures outside the physiological range (0 and 50 mm Hg). *Exp Eye Res*. 1975;20:523–530.
8. Grierson I, Lee WR. Light microscopic quantitation of the endothelial vacuoles in Schlemm's canal. *Am J Ophthalmol*. 1977;84:234–246.
9. Johnstone MA, Grant WG. Pressure-dependent changes in structures of the aqueous outflow system of human and monkey eyes. *Am J Ophthalmol*. 1973;75:365–383.
10. Lutjen-Drecoll E. Structural factors influencing outflow facility and its changeability under drugs. A study in Macaca arctoides. *Invest Ophthalmol*. 1973;12:280–294.
11. Ten Hulzen RD, Johnson DH. Effect of fixation pressure on juxtacanalicular tissue and Schlemm's canal. *Invest Ophthalmol Vis Sci*. 1996;37:114–124.
12. Rosenquist R, Epstein D, Melamed S, Johnson M, Grant WM. Outflow resistance of enucleated human eyes at two different perfusion pressures and different extents of trabeculotomy. *Curr Eye Res*. 1989;8:1233–1240.
13. Allingham RR, de Kater AW, Ethier CR. Schlemm's canal and primary open angle glaucoma: correlation between Schlemm's canal dimensions and outflow facility. *Exp Eye Res*. 1996;62:101–109.
14. Alvarado JA, Murphy CG. Outflow obstruction in pigmentary and primary open angle glaucoma. *Arch Ophthalmol*. 1992;110:1769–1778.
15. Forgáčová V, Lešták J, Pitrová S, Rozsival P. Schlemm's canal in OCT images in glaucoma patients and healthy subjects. *J Clin Exp Ophthalmol*. 2013;4:292.
16. Kagemann L, Wollstein G, Ishikawa H, et al. Identification and assessment of Schlemm's canal by spectral-domain optical coherence tomography. *Invest Ophthalmol Vis Sci*. 2010;51:4054–4059.
17. Chi HH, Katzin HM, Teng CC. Primary degeneration in the vicinity of the chamber angle; as an etiologic factor in wide-angle glaucoma. II. *Am J Ophthalmol*. 1957;43:193–203.
18. Dvorak-Theobald G. Further studies on the canal of Schlemm. Its anastomoses and anatomic relations. *Am J Ophthalmol*. 1955;39:65–89.
19. Teng CC, Paton RT, Katzin HM. Primary degeneration in the vicinity of the chamber angle; as an etiologic factor in wide-angle glaucoma. *Am J Ophthalmol*. 1955;40:619–631.
20. Battista SA, Lu Z, Hofmann S, Freddo T, Overby DR, Gong H. Reduction of the available area for aqueous humor outflow and increase in meshwork herniations into collector channels following acute IOP elevation in bovine eyes. *Invest Ophthalmol Vis Sci*. 2008;49:5346–5352.
21. Hann CR, Fautsch MP. Preferential fluid flow in the human trabecular meshwork near collector channels. *Invest Ophthalmol Vis Sci*. 2009;50:1692–1697.
22. Johnson DH. Histologic findings after argon laser trabeculoplasty in glaucomatous eyes. *Exp Eye Res*. 2007;85:557–562.

23. Melamed S, Epstein DL. Alterations of aqueous humour outflow following argon laser trabeculoplasty in monkeys. *Br J Ophthalmol*. 1987;71:776–781.
24. Svedbergh B. Protrusions of the inner wall of Schlemm's canal. *Am J Ophthalmol*. 1976;82:875–882.
25. Rohen J, Rentsch FJ. Electronmicroscopic studies on the structure of the outer wall of Schlemm's canal, its outflow channels and age changes. *Albrecht Von Graefes Arch Klin Exp Ophthalmol*. 1969;177:1–17.
26. Hann CR, Fautsch MP. The elastin fiber system between and adjacent to collector channels in the human juxtacanalicular tissue. *Invest Ophthalmol Vis Sci*. 2011;52:45–50.
27. Hann CR, Bentley MD, Vercnocke A, Ritman EL, Fautsch MP. Imaging the aqueous humor outflow pathway in human eyes by three-dimensional micro-computed tomography (3D micro-CT). *Exp Eye Res*. 2011;92:104–111.
28. Lutjen-Drecoll E, Futa R, Rohen JW. Ultrahistochemical studies on tangential sections of the trabecular meshwork in normal and glaucomatous eyes. *Invest Ophthalmol Vis Sci*. 1981;21:563–573.
29. Parc CE, Johnson DJ, Brilakis HS. Giant vacuoles are found preferentially near collector channels. *Invest Ophthalmol Vis Sci*. 2000;41:2984–2990.
30. Robb RA. The biomedical imaging resource at Mayo Clinic. *IEEE Trans Med Imaging*. 2001;20:854–867.
31. Rohen JW, Rentsch FJ. Uber den Bau des Schlemmschen Kanals und seiner AbfluBwege beim Menschen. *Albrecht Von Graefes Arch Klin Exp Ophthalmol*. 1968;176:309–329.
32. Bentley MD, Jorgensen SM, Lerman LO, Ritman EL, Romero JC. Visualization of three-dimensional nephron structure with microcomputed tomography. *Anat Rec (Hoboken)*. 2007;290:277–283.
33. Dvorak-Theobald G. Schlemm's canal: its anastomoses and anatomic relations. *Trans Am Ophthalmol Soc*. 1934;32:574–595.
34. Leber T. Der Circulus venosus Schlemmi steht nicht in offener Verbindung mit der vorderen Augenkammer. *Graefes Arch Clin Exp Ophthalmol*. 1895;41:235.
35. Hoffmann F, Dumitrescu L. Schlemm's canal under the scanning electron microscope. *Ophthal Res*. 1971;2:37–45.
36. Lee WR, Grierson I. Relationships between intraocular pressure and the morphology of the outflow apparatus. *Trans Ophthalmol Soc U K*. 1974;94:430–449.
37. Van Buskirk EM, Grant WM. Lens depression and aqueous outflow in enucleated primate eyes. *Am J Ophthalmol*. 1973;76:632–640.
38. Coleman DJ, Trokel S. Direct-recorded intraocular pressure variations in a human subject. *Arch Ophthalmol*. 1969;82:637–640.
39. Furuyoshi N, Furuyoshi M, Futa R, Gottanka J, Lutjen-Drecoll E. Ultrastructural changes in the trabecular meshwork of juvenile glaucoma. *Ophthalmologica*. 1997;211:140–146.
40. Last JA, Pan T, Ding Y, et al. Elastic modulus determination of normal and glaucomatous human trabecular meshwork. *Invest Ophthalmol Vis Sci*. 2011;52:2147–2152.

Investigative Ophthalmology & Visual Science